

Partitioned semi-implicit methods for simulation of biomechanical fluid-structure interaction problems

A Naseri, O Lehmkuhl, I Gonzalez and A Oliva

Heat and Mass Transfer Technological Centre (CTTC), Universitat Politècnica de Catalunya (UPC), ESEIAAT, Carrer de Colom 11, 08222 Terrassa (Barcelona), Spain

E-mail: anaseri@cttc.upc.edu

Abstract. This paper represents numerical simulation of fluid-structure interaction (FSI) system involving an incompressible viscous fluid and a lightweight elastic structure. We follow a semi-implicit approach in which we implicitly couple the added-mass term (pressure stress) of the fluid to the structure, while other terms are coupled explicitly. This significantly reduces the computational cost of the simulations while showing adequate stability. Several coupling schemes are tested including fixed-point method with different static and dynamic relaxation, as well as Newton-Krylov method with approximated Jacobian. Numerical tests are conducted in the context of a biomechanical problem. Results indicate that the Newton-Krylov solver outperforms fixed point ones while introducing more complexity to the problem due to the evaluation of the Jacobian. Fixed-point solver with Aitken's relaxation method also proved to be a simple, yet efficient method for FSI simulations.

1. Introduction

Fluid-structure interaction (FSI) refers to problems that deal with mutual interaction between fluid flow and a moving or deforming structure. Two different approaches could be taken to solve FSI problems, namely monolithic and partitioned approaches. Monolithic methods use a single solver to solve fluid and structural governing equations simultaneously. As the equations are solved together, the interaction between the domains is inherently taken into account. Partitioned methods, on the other hand, use separate solvers for fluid and structural equations and adopt a coupling scheme to account for the interaction of the domains. The coupling scheme determines the order and frequency in which the fluid and structural equations should be solved. It also determines the manner of communication and information exchange between the two solvers which is essentially restricted to the fluid-structure interface. The main advantage of the partitioned approach over monolithic one is using the most adapted numerical methods for each sub-problem domain which greatly increases the efficiency of the numerical solvers and the accuracy and reliability of the results [1].

Partitioned methods are further divided into loosely coupled (or explicit) and strongly coupled (or implicit) schemes. In loosely coupled schemes, the fluid and structural equations are solved in sequence and only once at every time step. Explicit methods work particularly well for aeroelastic problems or problems involving compressible viscous flow [2, 3]. Solving the fluid and structural equations only once at each time step, however, does not precisely satisfy the coupling condition at the fluid-structure interface. This makes the loosely coupled schemes unstable for a range of



problems especially ones with incompressible flow and high fluid/structure density ratios. It has been shown that instability is caused by the so called added-mass effect [4, 5].

Implicit schemes, in contrast, enforce the exact coupling condition by means of iterations between fluid and structural solvers at each time step. Jacobi and Gauss-Seidel iterations are the most basic implicit schemes that can be combined with different relaxation methods [1, 6]. Newton and quasi-Newton methods are also widely used to carry out the coupling iterations [7–9]. However, performing several coupling iterations at each time step significantly increases the computational cost of the FSI simulations. Semi-implicit methods try to mitigate this problem by splitting the fluid equations and applying implicit coupling only to the terms associated with the added-mass effect. This modification prevents excessive computational cost while maintaining the stability [10–12].

In this study, we follow a semi-implicit approach to solve FSI problem of an incompressible flow inside a deformable vessel, a test case in the context of blood flow inside arteries. The specific combination of physical parameters in this test case brings about a particularly challenging FSI problem due to a strong added-mass effect. Using a fractional step projection method allows us to separate the added-mass term and couple it implicitly to the structural solver. Two different family of solvers, namely fixed-point and Newton-Krylov solvers are used to solve the resulting interface problem. Results are represented and a comparison is made between performance of different methods.

2. Governing equations

In this section we provide the governing equations for both sub-domains of the problem. The fluid and structural domains will be referred to as Ω_f and Ω_s respectively. The interface of the domains will be denoted by $\Gamma_i = \Omega_f \cap \Omega_s$.

2.1. Fluid domain

The unsteady flow of an incompressible viscous fluid is governed by the Navier-Stokes equations. An Arbitrary Lagrangian-Eulerian (ALE) formulation of these equations to be solved on a moving mesh is given by:

$$\nabla \cdot \mathbf{u} = 0 \quad (1)$$

$$\frac{\partial \mathbf{u}}{\partial t} + (\mathbf{u} - \mathbf{w}) \cdot \nabla \mathbf{u} = -\frac{1}{\rho_f} \nabla p + \nu \Delta \mathbf{u} \quad (2)$$

where \mathbf{u} and p denote fluid velocity and pressure respectively, ρ_f is the fluid density, ν the kinematic viscosity and t is time. The velocity of the control volume's faces is denoted by \mathbf{w} .

The boundary condition for the fluid on the fluid-structure interface comes from the coupling condition:

$$\mathbf{u} = \frac{\partial \mathbf{d}}{\partial t} \quad \text{on } \Gamma_i \quad (3)$$

with \mathbf{d} representing the location of the interface. Appropriate boundary conditions should be provided on the rest of the fluid boundaries.

Before fluid equations could be solved, a moving mesh technique should be used to adapt the fluid mesh to the new location of the interface at each time step and evaluate the surface velocities \mathbf{w} . For the discretized equations to be conservative in time, the Space Conservation Law (SCL) should be satisfied while evaluating the surface velocities. SCL states that the volume swept by the surfaces of each control volume must be equal to the time rate of change of its volume v :

$$\frac{\partial v}{\partial t} - \int_{\partial v} \mathbf{w} \cdot d\mathbf{A} = 0 \quad (4)$$

where ∂v is the boundary of the control volume and \mathbf{A} is the area vector pointing outward.

The process of moving the fluid mesh and evaluating the surface velocities at a new time step t^{n+1} would be denoted by the function \mathbf{M} :

$$(\Omega_f^{n+1}, \mathbf{w}^{n+1}) = \mathbf{M}(\mathbf{d}^{n+1}) \quad (5)$$

The complete process of solving the fluid equations would then be concisely represented as:

$$\boldsymbol{\sigma}_i = \mathbf{F}(\mathbf{d}) \quad (6)$$

where $\boldsymbol{\sigma}_i$ stands for the fluid stress on the interface Γ_i . Given the current location of the interface \mathbf{d} , the fluid solver \mathbf{F} will adapt the fluid mesh accordingly and solve the fluid equations to obtain the velocity and pressure fields. In particular, velocity and pressure distribution on the interface will be used to calculate the fluid stress $\boldsymbol{\sigma}_i$, which will further be used by the structural solver.

2.2. Structural domain

The FSI problem to be considered in this work is the one of blood flow inside arteries. Thus the structural domain to be modeled is the vascular wall. Neglecting the anisotropic behaviour of the vascular wall and its circumferential deformation, it can be modeled by Navier's equations [13]:

$$\rho_s h \frac{\partial^2 D_r}{\partial t^2} - k G h \frac{\partial D_r}{\partial z^2} + \frac{E h}{1 - \xi^2} \left(\frac{\xi}{R_0} \frac{\partial D_z}{\partial z} + \frac{D_r}{R_0^2} \right) = \Phi_1 \quad (7)$$

$$\rho_s h \frac{\partial^2 D_z}{\partial t^2} - \frac{E h}{1 - \xi^2} \left(\frac{\xi}{R_0} \frac{\partial D_r}{\partial z} + \frac{\partial^2 D_z}{\partial z^2} \right) = \Phi_2 \quad (8)$$

in which $\mathbf{d} = [D_r, 0, D_z]^T$ is the displacements of the interface with respect to a reference state in the cylindrical coordinate (r, θ, z) . $R_0(z)$ denotes the vessel reference radius at rest, h is the wall thickness, k is the Timoshenko shear correction factor, G the shear modulus, E the Young modulus, ξ the Poisson ratio and ρ_s the density of the structure. The external force term is represented by $\boldsymbol{\sigma}_i = [\Phi_1, \Phi_2, 0]^T$ which is a function of fluid velocity and pressure distribution on the solid wet boundary $\boldsymbol{\sigma}_i = \boldsymbol{\sigma}_i(\mathbf{u}, p)_{\Gamma_i}$.

In this study we will use a more simplified model for the vessel wall, assuming that the force term $\boldsymbol{\sigma}_i$ is due to the fluid pressure only and also neglecting the longitudinal deformation of the wall. These further assumptions (also suggested in [13] and used in [14, 15]) will reduce the wall model into a single PDE equation given by:

$$\rho_s h \frac{\partial^2 \mathbf{d}}{\partial t^2} - k G h \frac{\partial^2 \mathbf{d}}{\partial z^2} + \frac{E h}{1 - \xi^2} \frac{\mathbf{d}}{R_0^2} = \boldsymbol{\sigma}_i \quad (9)$$

where $\mathbf{d} = [D_r, 0, 0]^T$ and $\boldsymbol{\sigma}_i = [\Phi_1, 0, 0]^T$. The structural solver then could be represented as:

$$\mathbf{d} = \mathbf{S}(\boldsymbol{\sigma}_i) \quad (10)$$

Given the current fluid stress on the wet boundary, the structural solver \mathbf{S} will solve the equation 9 to obtain the new location of the interface.

3. Semi-implicit coupling approach

Defining the fluid and structural equations concisely as equations 6 and 10, will reduce the coupled fluid-structure system of equations into an interface problem of the form:

$$\mathbf{S} \circ \mathbf{F}(\mathbf{d}) - \mathbf{d} = 0 \quad (11)$$

with \mathbf{d} and functions \mathbf{F} and \mathbf{S} , all in the new time step t^{n+1} . In an implicit coupling approach, equation 11 would be solved iteratively at each time step until a predefined convergence criterion is met. In this study we will follow a semi-implicit approach which is coupling only the pressure stress term of the fluid, implicitly to the structure, while the rest of the terms are coupled explicitly. Pressure stress term is responsible for the added-mass effect and coupling this term explicitly will cause numerical instability [4]. By implicitly coupling the pressure stress term, stability problems could be alleviated while explicitly coupling the other terms would save a significant computational cost. This idea was first proposed in [10] and later used in [11, 12].

The pressure stress term is split off by using a fractional step projection method for fluid flow equations. The method, described in detail in [16], along with an explicit time advancement yields to a three step solution procedure for the equations 1 and 2:

$$\mathbf{u}^p = \mathbf{u}^n - \Delta t[(\mathbf{u}^n - \mathbf{w}).\nabla\mathbf{u}^n - \nu\Delta\mathbf{u}^n] \quad (12)$$

$$\frac{\Delta t}{\rho_f}\Delta p^{n+1} = \nabla \cdot \mathbf{u}^p \quad (13)$$

$$\mathbf{u}^{n+1} = \mathbf{u}^p - \frac{\Delta t}{\rho_f}\nabla p^{n+1} \quad (14)$$

with \mathbf{u}^p denoting the predicted velocity. The velocity predictor step (equation 12) which contains the fluid convective and diffusive terms, will be coupled explicitly to the structure. In contrast to reference [10] that implicitly couples both pressure equation (equation 13) and velocity correction (equation 14) steps, we shall only implicitly couple the pressure equation. So the process of solving the full coupled problem at each time step will be as follows:

step 0: extrapolating \mathbf{d} :

$$\tilde{\mathbf{d}}^{n+1} = 2.5\mathbf{d}^n - 2\mathbf{d}^{n-1} + 0.5\mathbf{d}^{n-2} \quad (15)$$

step 1: moving the fluid mesh (explicit coupling):

$$(\Omega_f^{n+1}, \mathbf{w}^{n+1}) = \mathbf{M}(\tilde{\mathbf{d}}^{n+1}) \quad (16)$$

step 2: velocity prediction (explicit coupling):

$$\mathbf{u}^p = \mathbf{u}^n - \Delta t[(\mathbf{u}^n - \mathbf{w}^{n+1}).\nabla\mathbf{u}^n - \nu\Delta\mathbf{u}^n] \quad \text{in } \Omega_f^{n+1} \quad (17)$$

step 3: pressure equation and structural solver (implicit coupling with k denoting the coupling iteration index):

$$\mathbf{u}_k^p = \frac{\mathbf{d}_k^{n+1} - \mathbf{d}^n}{\Delta t} \quad \text{on } \Gamma_i^{n+1} \quad (18)$$

$$\frac{\Delta t}{\rho_f}\Delta p_k^{n+1} = \nabla \cdot \mathbf{u}_k^p \quad \text{in } \Omega_f^{n+1} \quad (19)$$

$$\boldsymbol{\sigma}_{i_k} = \boldsymbol{\sigma}_i(p_k^{n+1}) \quad \text{on } \Gamma_i^{n+1} \quad (20)$$

$$\mathbf{d}_{k+1}^{n+1} = \mathbf{S}(\boldsymbol{\sigma}_{i_k}) \quad \text{on } \Gamma_i^{n+1} \quad (21)$$

step 4: velocity correction (explicit coupling):

$$\mathbf{u}^{n+1} = \mathbf{u}^p - \frac{\Delta t}{\rho_f}\nabla p^{n+1} \quad \text{in } \Omega_f^{n+1} \quad (22)$$

$$\mathbf{u}^{n+1} = \frac{\mathbf{d}^{n+1} - \mathbf{d}^n}{\Delta t} \quad \text{on } \Gamma_i^{n+1} \quad (23)$$

With this semi-implicit coupling approach, the FSI interface problem (equation 11) is modified to:

$$\mathbf{R}(\mathbf{d}) = \mathbf{S} \circ \mathbf{f}(\mathbf{d}) - \mathbf{d} = 0 \quad (24)$$

which stands for the step 3 of the above algorithm. In the new FSI equation, instead of full fluid solver function \mathbf{F} , only the pressure equation (denoted by \mathbf{f}) is coupled to the structure implicitly. Again \mathbf{d} and the functions \mathbf{f} and \mathbf{S} , all are in the new time step t^{n+1} . In the next chapter we will explain the solution methods to resolve the equation 24.

4. Coupling schemes

In this section we will discuss two family of solvers to solve the nonlinear FSI interface problem (equation 24), namely fixed-point and Newton-Krylov solvers.

4.1. Fixed-point solvers

This is a class of iterative solvers that are popular mostly for their simplicity. Jacobi and Gauss-Seidel iterations are the most basic and popular forms. A block Gauss-Seidel method is used in this study. Each iteration begins with solving the coupled system:

$$\tilde{\mathbf{d}}_{k+1} = \mathbf{S} \circ \mathbf{f}(\mathbf{d}_k) \quad (25)$$

where k indicates the coupling iterations. The index $n + 1$ is dropped because all the parameters are at the same time step. The interface residual is defined as:

$$\mathbf{r}_{k+1} = \mathbf{R}(\mathbf{d}_k) = \tilde{\mathbf{d}}_{k+1} - \mathbf{d}_k \quad (26)$$

FSI convergence is achieved at every time step when the 2-norm of the interface residual is small enough to meet the predefined convergence criterion. It has been shown in several works that Gauss-Seidel scheme either converges very slowly or does not converge at all for FSI problems involving incompressible flow. Our own tests proved this method to be unstable for the problem in hand. To alleviate the convergence problem of the Gauss-Seidel method, a static or dynamic relaxation is needed:

$$\mathbf{d}_{k+1} = \mathbf{d}_k + \omega_k \mathbf{r}_{k+1} \quad (27)$$

The relaxation factor ω is evaluated in three different ways:

1- *Fixed relaxation factor*: a fixed value is assigned for all iterations. This value should be adjusted for each problem to be small enough to keep the solution stable during whole simulation. It also should not be too small to avoid excessive unnecessary iterations.

2- *Aitken's dynamic relaxation method*: Aitken's Δ^2 method uses values from two previous iterations to enhance the current step. For a vector equation, ω_k could be obtained by [17]:

$$\omega_k = -\omega_{k-1} \frac{\mathbf{r}_k^T (\mathbf{r}_{k+1} - \mathbf{r}_k)}{|\mathbf{r}_{k+1} - \mathbf{r}_k|^2} \quad (28)$$

3- *Steepest descent method*: This method is based on taking the optimal step length at \mathbf{r}_{k+1} direction so that the next residual vector is orthogonal to the current one. An approximated way of calculating the relaxation factor based on this idea is proposed by [6] as:

$$\omega_k = \frac{\mathbf{r}_{k+1}^T \mathbf{r}_{k+1}}{\mathbf{r}_{k+1}^T \mathbf{R}'(\mathbf{d}_k) \mathbf{r}_{k+1}} \quad (29)$$

where \mathbf{R}' is Jacobian of \mathbf{R} . Normally, the Jacobian matrix of the coupled system of fluid-structure equations is not easily accessible. The product of the Jacobian matrix and a vector \mathbf{v} could be evaluated by a first order Taylor series approximation:

$$\mathbf{R}'(\mathbf{d}_k)\mathbf{v} = \frac{\mathbf{R}(\mathbf{d}_k + \delta\mathbf{v}) - \mathbf{R}(\mathbf{d}_k)}{\delta} \quad (30)$$

where δ is a sufficiently small value ($\delta = 10^{-6}$ has shown adequate accuracy and is used in this study).

4.2. Newton-Krylov solvers

This method consists of two levels of iterative solvers. First level is Newton's method for linearizing the problem and the second level is a Krylov subspace solver to solve the resulting linear system of equations. In order to apply the Newton's method to the nonlinear interface problem (equation 24), the interface residual is defined similarly by equation 26 while the line search step of the fixed-point method (equation 27) is replaced by:

$$\mathbf{R}'(\mathbf{d}_k)\Delta\mathbf{d}_{k+1} = -\mathbf{R}(\mathbf{d}_k) \quad (31)$$

$$\mathbf{d}_{k+1} = \mathbf{d}_k + \Delta\mathbf{d}_{k+1} \quad (32)$$

Since the Jacobian matrix of the coupled system of fluid-structure equations is not easily accessible, a Jacobian-free Krylov subspace solver could be used to solve the inner system of equations (equation 31). The product of the Jacobian matrix and a vector is similarly approximated by the equation 30. A GMRES solver [18] without preconditioner is used in this study as the inner Krylov solver. A survey on Jacobian-free Newton-Krylov methods and their considerations could be found at [19].

5. Numerical tests

Numerical tests are conducted on a benchmark problem proposed by [15] and studied, among others, by [6, 8, 20, 21]. The problem is a 3D flow inside a deformable tube which is motivated by the type of problems faced in hemodynamics. The tube has a length of $l = 0.05\text{m}$, an inner diameter of $r_i = 0.005\text{m}$ and a wall thickness of $h = 0.001\text{m}$. The structural density is $\rho_s = 1200\text{kg/m}^3$, the Young modulus $E = 3 \times 10^5\text{N/m}^2$ and the Poisson ratio $\xi = 0.3$. The Timoshenko factor is set to $k = 5/6$. The fluid density and viscosity are $\rho_f = 1000\text{kg/m}^3$ and $\mu_f = 0.003\text{Pa} \cdot \text{s}$, respectively. The tube is clamped at both ends and the fluid is initially at rest. A pressure of 1333.2Pa is applied at the tube inlet during a period of 0.003s and 0Pa after. Pressure at the outlet is set to 0Pa during whole simulation. Simulations are carried out during 0.01 s with time steps of 0.0001 s .

Finite-volume method is used for spatial discretization of both fluid and structural equations. Second-order symmetry-preserving schemes are used for fluid equations. The in-house fluid solver code and the numerical methods are described in detail in [16, 22]. Second-order central-difference spatial discretization scheme along with implicit time integration is used for structural equation. The fluid mesh is unstructured and consists of 2.1×10^4 control volumes with 3.5×10^3 nodes on the fluid-structure interface which is also used as solid mesh. Moving mesh technique is explained at [23].

The propagation of the pressure wave inside the vessel is observed. Figure 1 shows pressure contour plots at three different times: $t=0.0025, 0.005$ and 0.0075 s . Deformation of the interface is magnified by a factor of 10 to be visible more clearly. Results are in a good agreement with those of [6, 8, 20, 21].

Three of the four coupling schemes were able to secure FSI convergence at each time step and they all converged to the same solution. The fixed-point method with steepest-descent relaxation

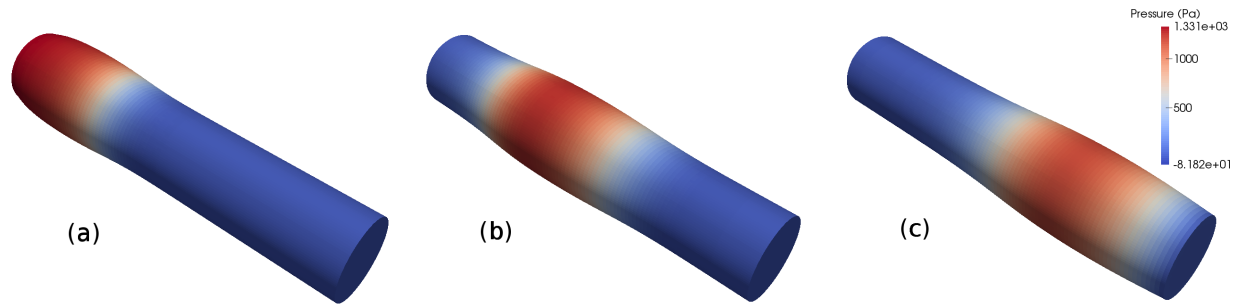


Figure 1. Pressure wave propagation inside the deformable vessel: (a) $t=0.0025s$, (b) $t=0.005s$ and (c) $t=0.0075s$.

technique failed to converge at every time step and was found to be an inadequate method for the current problem. Table 1 contains performance criteria of the three stable coupling methods. It indicates the average number of coupling iterations each scheme requires to converge. It also contains the frequency at which the coupled system of fluid-structure equations, $\mathbf{S} \circ \mathbf{f}(\mathbf{d})$, must be solved at each time step. These two criteria are essentially identical for the two fixed-point schemes but vary for Newton-Krylov method, because it undergoes an inner loop inside every coupling iteration. The actual CPU time for the simulations are also presented in the table, normalized by the smallest one which is that of Newton-Krylov method.

Table 1. Performance comparison of different coupling schemes.

Coupling scheme	Average No. of FSI iterations	Average Frequency of system solution	relative CPU time
Fixed-point (const. relax.)	389.7	389.7	7.51
Fixed-point (Aitken)	55.6	55.6	1.07
Newton-Krylov	3.2	45.2	1.00

Newton-Krylov method has proved the most efficient coupling scheme based on computational time. Aitken's method, which is a less complicated method in terms of implementation, also shows a good performance and takes only 7% more CPU time. Comparing two fixed-point schemes, it is seen that Aitken's dynamic relaxation method reduces the average number of coupling iterations dramatically. The required computational time is also decreased by the same rate.

Both Aitken's and Newton-Krylov methods show a favorable performance and stability. Although Newton-Krylov method secures convergence in a far less number of iterations, the average frequency of solving the coupled equations is not hugely different from that of Aitken's method, and so is the computational time. This fact is highlighted in figures 2 and 3 which compare, respectively, the number of coupling iterations and CPU time each method needs to converge at each time step. CPU times are normalized by the average CPU time Newton-Krylov method takes for one time step.

It is worth reminding that no preconditioner is used for the GMRES solver of the Newton-Krylov method in this work. Performance of Krylov subspace solvers can be significantly boosted by using a preconditioner. However, designing a matrix-free preconditioner that can use the approximated Jacobian of the system is not straightforward.

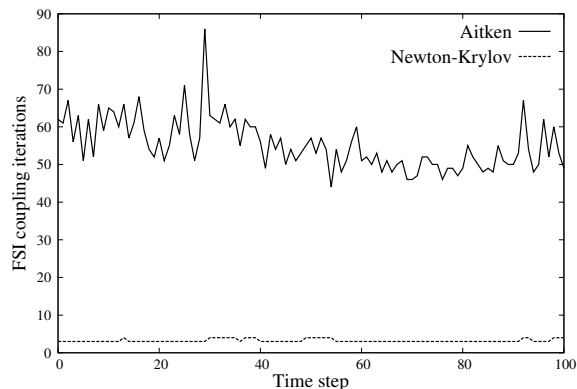


Figure 2. Number of FSI coupling iterations required for each coupling scheme

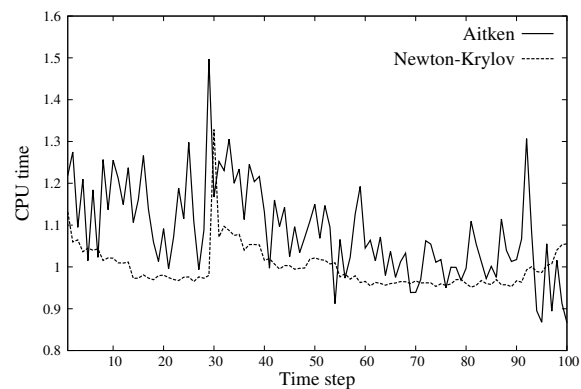


Figure 3. CPU time required for each coupling scheme

6. Conclusions

A semi-implicit approach is followed to solve FSI problem of an incompressible flow inside a deformable vessel. Only the pressure stress term of the fluid is coupled implicitly to the structure and adequate stability is seen in a test case with strong added-mass effect. Four different coupling schemes are tested including three fixed-point solvers with constant, Aitken's and steepest descent relaxations as well as one Newton-Krylov solver with approximated Jacobian. The fixed-point solver with steepest-descent relaxation failed to achieve FSI convergence at every time step and was found inadequate for the current problem. The other three schemes showed proper stability, although constant relaxation scheme had a very poor performance. Both Aitken's and Newton-Krylov methods are found to be efficient for the current FSI simulations, with Newton-Krylov method being slightly faster and Aitken's method being easier to implement.

References

- [1] Degroote J 2013 *Arch. Comput. Methods Eng.* **20** 185–238
- [2] Farhat C, Van der Zee K G and Geuzaine P 2006 *Comput. Methods Appl. Mech. Eng.* **195** 1973–2001
- [3] Van Brummelen E 2009 *J. Appl. Mech.* **76** 021206
- [4] Causin P, Gerbeau J F and Nobile F 2005 *Comput. Methods Appl. Mech. Eng.* **194** 4506–4527
- [5] Förster C, Wall W A and Ramm E 2007 *Comput. Methods Appl. Mech. Eng.* **196** 1278–1293
- [6] Küttler U and Wall W a 2008 *Comput. Mech.* **43** 61–72
- [7] Michler C, Van Brummelen E and De Borst R 2005 *Int. J. Numer. Methods Fluids* **47** 1189–1195
- [8] Fernández M Á and Moubachir M 2005 *Comput. Struct.* **83** 127–142
- [9] Gerbeau J F, Vidrascu M and Frey P 2005 *Comput. Struct.* **83** 155–165
- [10] M A Fernández J F G and Grandmont C 2007 *Int. J. Numer. Methods Eng.* 794–821 (*Preprint* 1010.1724)
- [11] Quaini A and Quarteroni A 2007 *Math. Model. Methods Appl. Sci.* **17** 957–983
- [12] Breuer M, De Nayer G, Münsch M, Gallinger T and Wüchner R 2012 *J. Fluids Struct.* **29** 107–130
- [13] Quarteroni A, Tuveri M and Veneziani A 2000 *Comput. Vis. Sci.* **2** 163–197
- [14] Gerbeau J F and Vidrascu M 2003 *ESAIM Math. Model. Numer. Anal.* **37** 631–647
- [15] Formaggia L, Gerbeau J F, Nobile F and Quarteroni A 2001 *Comput. Methods Appl. Mech. Eng.* **191** 561–582
- [16] Jofre L, Lehmkuhl O, Ventosa J, Trias F X and Oliva A 2014 *Numer. Heat Transf. Part B Fundam.* **65** 53–79
- [17] Irons B M and Tuck R C 1969 *Int. J. Numer. Methods Eng.* **1** 275–277
- [18] Saad Y and Schultz M H 1986 *SIAM J. Sci. Stat. Comput.* **7** 856–869
- [19] Knoll D a and Keyes D E 2004 *J. Comput. Phys.* **193** 357–397
- [20] Degroote J and et al 2010 *Int. J. Numer. Method. Biomed. Eng.* **26** 276–289
- [21] Küttler U and et al 2010 *Int. J. Numer. Method. Biomed. Eng.* **26** 305–321
- [22] Lehmkuhl O and et al 2009 *Parl. Comput. Fluid Dyna. 2007* (Springer) pp 275–282
- [23] Estruch O, Lehmkuhl O, Borrell R, Segarra C D P and Oliva a 2013 *Comput. Fluids* **80** 44–54